



A novel A-D-A small molecule with 1,8-naphthalimide as a potential non-fullerene acceptor for solution processable solar cells

Mengmeng Zhu ^a, Jingsheng Miao ^a, Zhao Hu ^a, Yantong Chen ^a, Ming Liu ^a, Imran Murtaza ^{b,c}, Hong Meng ^{a,*}

^a School of Advanced Materials, Peking University Shenzhen Graduate School, Shenzhen 518055, China

^b Key Laboratory of Flexible Electronics (KLOFE) & Institute of Advanced Materials (IAM), Jiangsu National Synergetic Innovation Center for Advanced Materials (SICAM), Nanjing Tech University (Nanjing Tech), 30 South Puzhu Road, Nanjing 211816, China

^c Department of Physics, International Islamic University, Islamabad 44000, Pakistan

ARTICLE INFO

Article history:

Received 18 January 2017

Received in revised form

6 March 2017

Accepted 6 March 2017

Available online 8 March 2017

Keywords:

Organic solar cell

Non-fullerene acceptor

1,8-Naphthalimide (NI)

Perylene diimide (PDI)

ABSTRACT

In this work, the structure-property relationship of fused-ring electron acceptors is briefly discussed and the principle of molecular design is presented. Based on this principle, perylene diimide (PDI) was cracked by inserting thiophene and thieno[3,2-*b*]thiophene (TT) to design and synthesize a novel A-D-A (acceptor-donor-acceptor) small molecule DNIT-TT2T, which served as a non-fullerene acceptor material in our fabricated organic solar cells (OSCs). DNIT-TT2T shows excellent thermal stability, it possesses a broad absorption by covering the wavelength range of 300–600 nm and relatively high LUMO energy level of −3.75 eV, which is close to the theoretically calculated value. The power conversion efficiency (PCE) of OSCs based on the blend of P3HT donor and DNIT-TT2T acceptor (1:1, w/w) is found to be 1.25%, with a high open-circuit voltage (V_{oc}) of 0.88 V, indicating that 1,8-naphthalimide (NI) based molecules are promising acceptors for non-fullerene polymer solar cells and excellent photovoltaic properties can be achieved by rationally designing the molecules.

© 2017 Elsevier Ltd. All rights reserved.

1. Introduction

In recent years, solution-processed bulk heterojunction (BHJ) polymer solar cells (PSCs) have attracted intensive attention both from academicians and industrialists, because of their noteworthy merits, such as eco-friendly energy source, light weight, cost-effective, ease of large-area fabrication by roll-to-roll printing and considerable solar energy conversion efficiency [1–4]. In general, fullerenes and its derivatives have been extensively used as acceptor materials in a vast majority of efficient organic photovoltaic (OPV) systems due to their special advantages such as high electron mobility, isotropic charge transfer and transport, as well as formation of appropriate phase separation [5,6]. Currently, state-of-the-art PSCs based on fullerene acceptors have achieved power conversion efficiencies (PCEs) up to 10–11% [7–9]. High-performance solar cells modified by porous conjugated polymer thin films have been fabricated recently and a promising future is expected [10–13]. Despite significant success, fullerenes still have

some vital shortcomings hindering their application in OPVs, such as relatively weak absorption in the visible region, high cost, difficulty in tuning optical and electronic properties and instability in air [14,15]. To overcome these disadvantages, considerable efforts have been devoted to the design and synthesis of small molecule acceptors which can replace fullerenes and its derivatives. Compared with fullerenes, the small molecule acceptors have broader absorption, better stability, improved solubility and simple tunability of their molecular orbital energy level to match a range of donor polymers [16–21]. A-D-A (acceptor-donor-acceptor) structured small molecules which are easily synthesized and show good performance attract much attention [19,22,23]. Rhodanine [19,24], benzothiadiazole (BT) [19,24], perylene diimide (PDI) [25], naphthalene diimide (NDI) [26], cyano group [27], diketopyrrolopyrrole (DPP) [28] etc. are always used as the electron withdrawing groups when choosing building blocks to construct non-fullerene acceptors. Polycyclic fused ring system is always selected as donor unit, such as fluorine [24], indacenodithiophene (IDT) [29], indacenodithieno[3,2-*b*]thiophene (IT) [27] and their derivatives.

Fused-ring electron acceptors based on 5-heterocyclic ring IDT core have achieved some great achievements (Chart 1). IC-C6IDT-IC,

* Corresponding author.

E-mail address: menghong@pkusz.edu.cn (H. Meng).

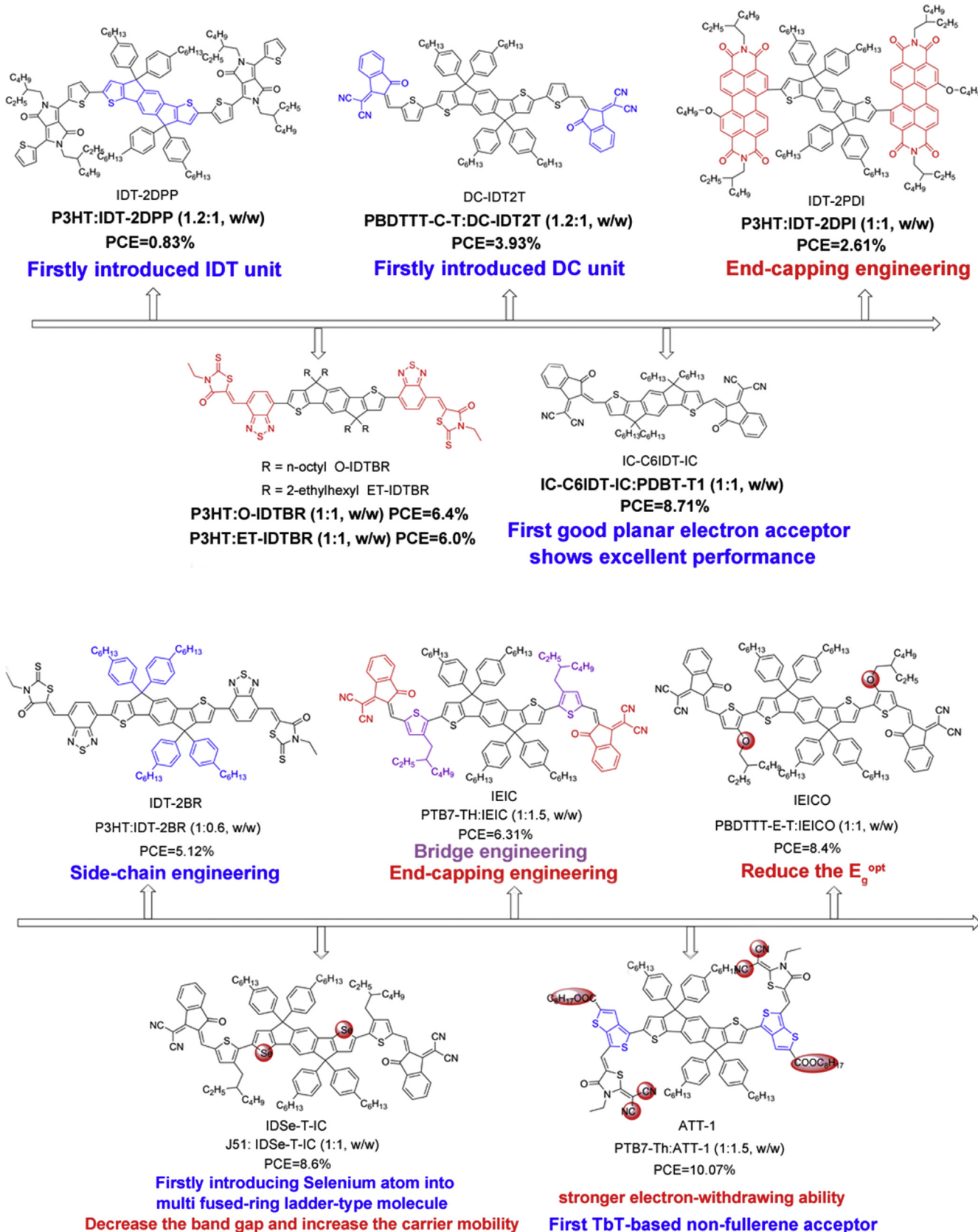


Chart 1. The brief progress of fused-ring electron acceptors based on IDT core [19,22,29,38–44].

a planar 5-heterocyclic ring electron acceptor, was designed and synthesized by Zhan et al. The device based on IC-C6IDT-IC:PDBT-

T1 (1:1, w/w) without additional treatment exhibited a high PCE of 8.71%. This result demonstrates that planar fused-ring electron

acceptors should deserve more attention [22].

Since Zhan et al. reported ITIC acceptor based 7-heterocyclic ring core in 2015, with the PCE of PSCs based on PTB7-TH:ITIC (1:1.3, w/w) films as high as 6.8%, this small molecule acceptor immediately attracted great attention [27]. Many polymer donors:ITIC-based PSCs have been investigated and have shown great performance [23,30–33]. In order to fine tune the bandgap, elevate the HOMO level, get higher mobility, and further match with more donor polymers, a series of ITIC derivatives (**Chart 2**) were designed and synthesized by the following techniques, **Chart 3** shows the structures of the donor polymers mentioned in this section.

- (i) The end-capping engineering: IT-DM and IT-M were synthesized by Hou's group [34]. Methyl, a small electron donating substituent, was introduced into the end-capping group to slightly lift up the LUMO level, without bringing in too much steric hindrance. The PCE of the device based on PBDB-T:IT-M (1:1, w/w) achieved 12.05%, which is the highest value among single-junction PSCs.
- (ii) The aromatic core engineering: Aromatic core of ITIC was modified by constructing multi fused-ring ladder-type conjugated unit (IDTIDT-IC) by Liao et al., the PCE of 6.48% based PTB7-TH:ITIC (1:1.5, w/w) was obtained with a low energy loss of 0.59 eV [35], a high V_{oc} of 0.94 V and a high EQE of 63%.
- (iii) The aromatic side-chain engineering: In order to lower the energy level, facilitate π stacking and charge transport, thiophene unit was introduced and ITIC-Th was synthesized by Zhan et al. which can be compatible with more high-performance donors, the devices based on PDBT-T1:ITIC-Th

(1:1, w/w) yielded PCE as high as 9.6% [18]. The isomer *m*-ITIC was synthesized by changing the position of meta-alkyl-phenyl substitution and the PCE of the devices based on J61:*m*-ITIC (1:1, w/w) reached up to 11.77% which is higher than that of the device based on ITIC (10.57%) [36]. Moreover, the devices based on FDICTF:PBDB-T (1.2:1, w/w) yielded a high PCE of 10.06% [37].

Here we propose the design principle of fused-ring electron acceptor (**Scheme 1**) based on the following facts:

- (i) The fused-ring core and end-capping electron withdrawing group mainly determine the highest occupied molecular orbital (HOMO) and lowest unoccupied molecular orbital (LUMO) energy levels.
- (ii) The aromatic fused ring core mainly determines the intermolecular charge transport.
- (iii) The LUMO energy level and the absorption in the visible and near infar-red (NIR) region can be mainly tuned by selecting acceptor units judiciously.
- (iv) The side chain mainly tune the solubility, crystallinity and morphology in BHJ blend films.
- (v) The bridges assist charge transport, band gap, absorption, solubility, crystallinity morphology and other properties.

As an n-type acceptor material, perylene diimide (PDI) derivatives have good light-harvesting property, strong electron-accepting properties and easy to form thinner films than fullerene derivatives [21,45–47], so the use of star-shaped PDI and its derivatives in organic electronics is a technical imperative

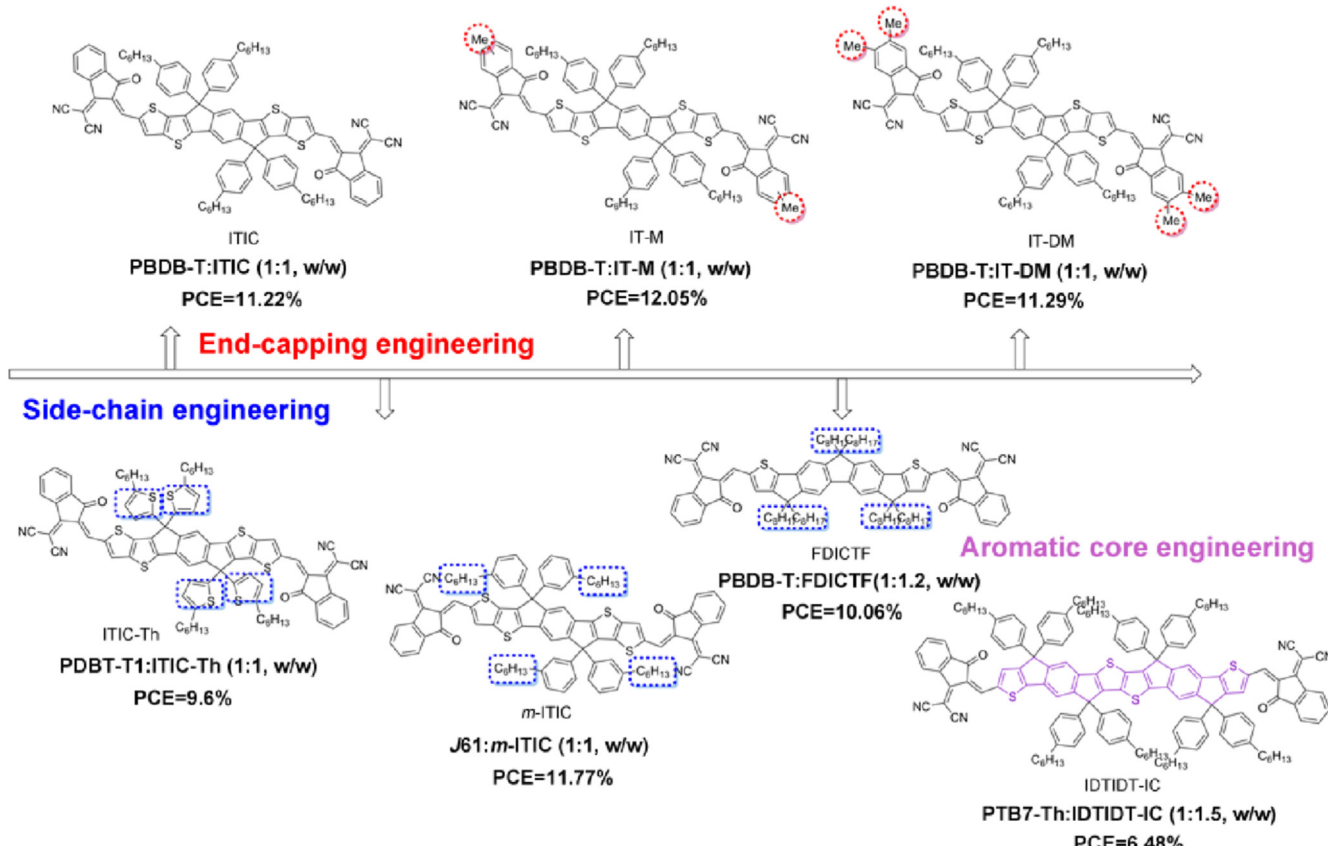


Chart 2. Chemical structures of ITIC and its derivatives.

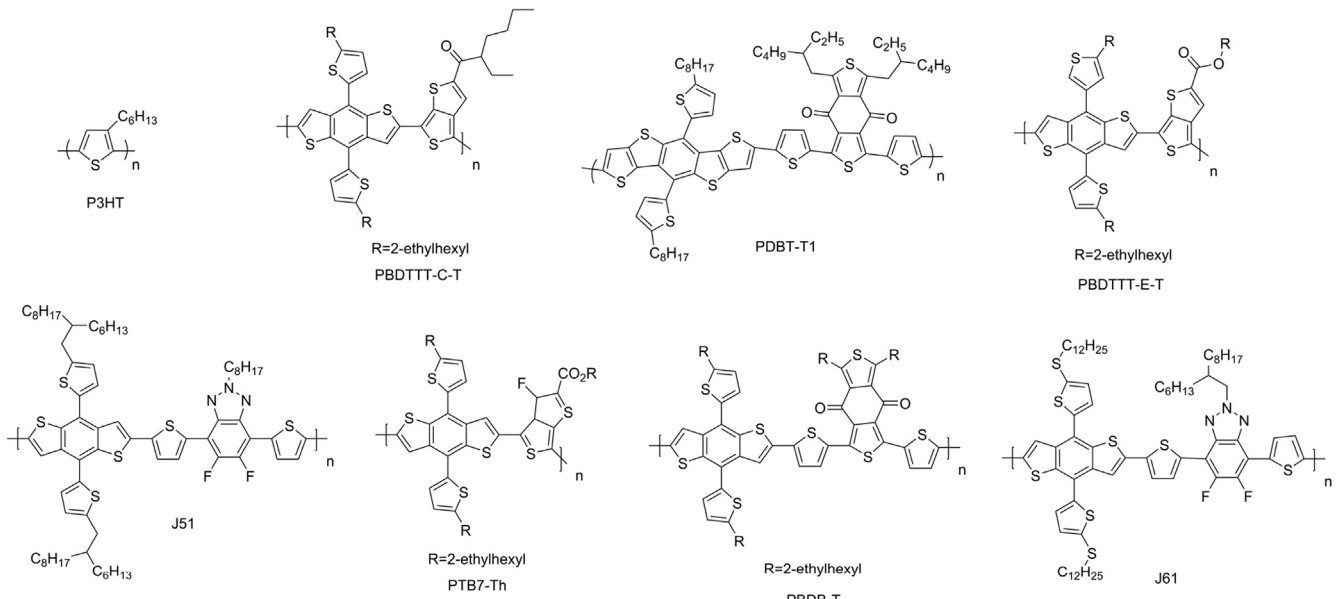
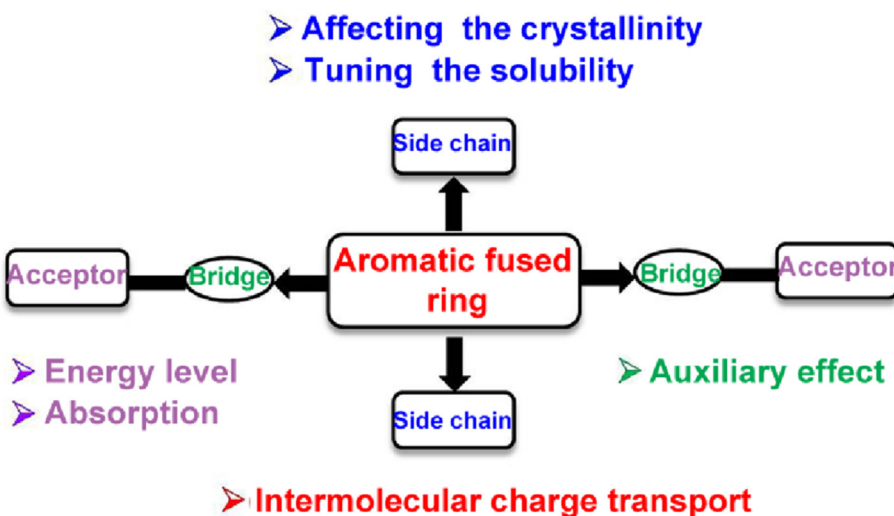


Chart 3. Chemical structures of all donor polymers used in polymer solar cells discussed in this section.

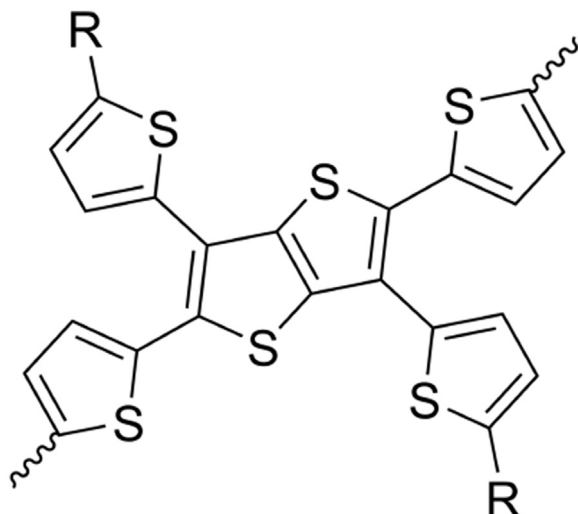


Scheme 1. Design principle of A-D-A non-fullerene acceptor.

[47–54]. However, PDI has an intrinsic drawback of inherent crystallinity so it cannot be blended with most of the donor materials. Therefore, to overcome its shortcoming, a series of PDI derivatives have been synthesized by cracking PDI unit and inserting conjugation moiety [55–60]. Moreover, small molecules containing 1,8-naphthalimide (NI) structure have higher lowest unoccupied molecular orbital (LUMO) level, which can easily produce higher V_{oc} and can also avoid the shortcoming of PDI derivatives [56]. But NI derivatives do not exhibit higher electron mobility, therefore, herein we introduce thiophene and thieno[3,2-*b*]thiophene substitution in PDI molecule. Thiophene and thieno[3,2-*b*]thiophene have been widely used in organic thin film transistors (OTFT) [61], organic photovoltaic cells (OPV) [62] organic light emitting diodes (OLED) [63,64], and display excellent performance. They can enlarge the effective π -conjugated backbone by appending conjugated thiophene side chain which can afford much broader absorption, improved charge mobility and reduced HOMO energy

level to perk up the fill factor (FF) and PCE. Thus we introduce a new core T-TT2T (**Scheme 2**) and use density functional theory (DFT) method (B3LYP/6-31G(d)) to investigate the HOMO, LUMO and band gap of different cores (**Scheme 3**).

A new two dimensional (2D) acceptor-donor-acceptor (A-D-A) type material, **DNIT-TT2T**, was further designed and synthesized (**Chart 4**). Comprised of thiophene and thieno[3,2-*b*]thiophene embedded between PDI unit, which displayed good solubility in common organic solvents at room temperature, such as dichloromethane and chloroform due to the presence of alkyl chains. Poly(3-hexylthiophene) (P3HT) is an economical donor which is widely used in novel non-fullerene PSCs [24,41,65]. P3HT possesses great potential to fabricate low-cost and high efficient PSCs due to its low-cost and easy-processing properties. We use the designed **DNIT-TT2T** as acceptor and benchmark poly(3-hexylthiophene) (P3HT) as donor to fabricate the bulk heterojunction solar cells. Herein, we thoroughly investigate the thermal stability, optical

**Scheme 2.** The structure of T-TT2T core.

properties, electrochemical properties and morphology of **DNIT-TT2T** thin films and fabricate PSCs based on DNIT-TT2T:P3HT (1:1, w/w) which exhibit PCE of 1.25% and a high V_{oc} of 0.88 V.

2. Experimental

2.1. General

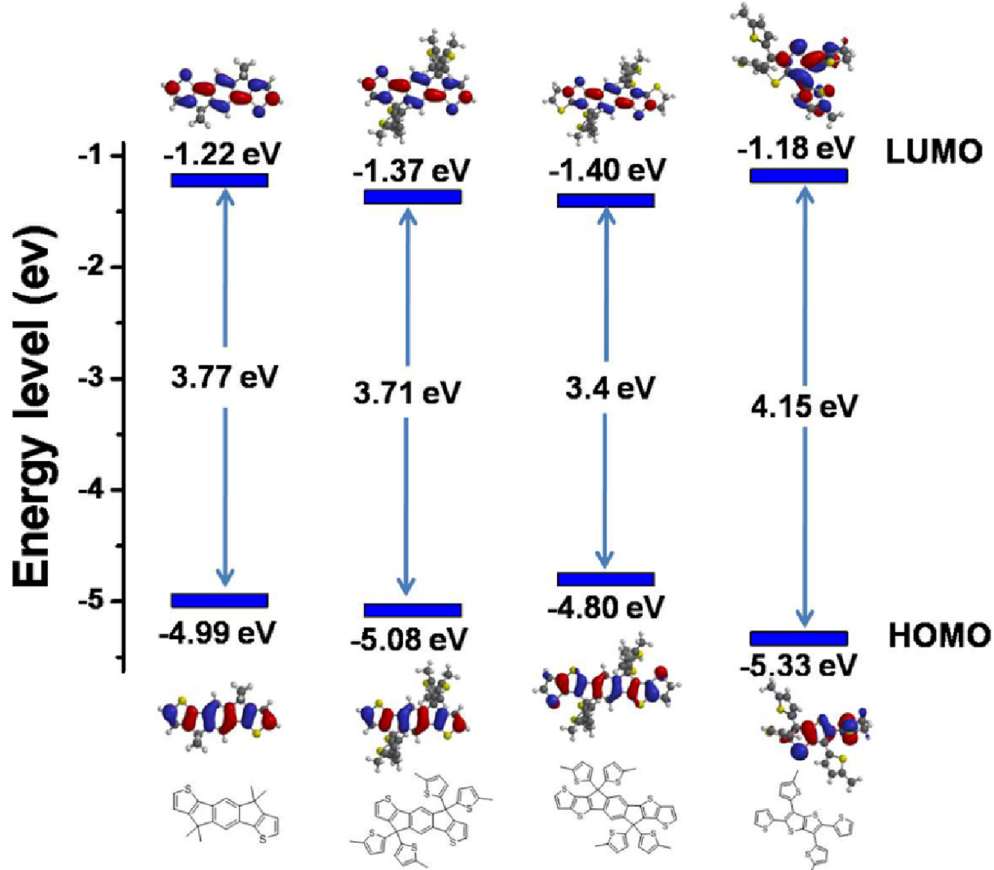
^1H and ^{13}C NMR spectra were recorded on a BrukerDM300

spectrometer using CDCl_3 as the solvent. Cyclic voltammetry (CV) was performed on a CHI620E electrochemical workstation and UV–Vis–NIR spectra were recorded using a Lambda 750 spectrophotometer. High resolution mass spectra were obtained from a MALDI-TOF Mass Spectrometer. Thermo-gravimetric analysis (TGA) was carried out with a Mettler-Toledo TGA thermal analyzer under purified nitrogen gas flow with a $10\text{ }^\circ\text{C min}^{-1}$ heating rate. Infrared (IR) spectra were recorded on PerkinElmer Frontier. Elemental analyses were performed on Elementar Vario MICRO (Germany). The morphology was studied by using Atomic Force Microscope (Bruker Multimode 8) and all images were obtained using typical parameters for tapping mode imaging.

2.2. Materials

All reagents and starting materials, unless otherwise specified, were purchased from commercial suppliers and used as received. Solvents were dried using standard procedures. All reactions were performed under an atmosphere of nitrogen. As outlined in **Scheme 4**, **compounds 1, 2, 5** and **8** were synthesized according to the reported procedures [66–69] and the new **compound 9** was synthesized by Stille coupling reaction according to the following details:

Compound 9 (DNIT-TT2T) was synthesized according to the same procedure as that for **compound 3** using **compound 7** (0.3 g, 0.25 mmol), **compound 8** (0.19 g, 0.5 mmol), anhydrous toluene (2.5 ml), tetrakis(triphenylphosphine)palladium (0) [$\text{Pd}(\text{PPh}_3)_4$] (12 mg). The crude product was purified by column chromatograph using petroleum ether and dichloromethane solution (2:1 by vol.) as eluent to give **compound 9** as an orange solid (0.27 g, 87%). ^1H

**Scheme 3.** DFT B3LYP/6-31G* optimized geometries of cores (hexyl group is substituted by methyl group for clarity of representation) (color online).

Inserting conjugation units

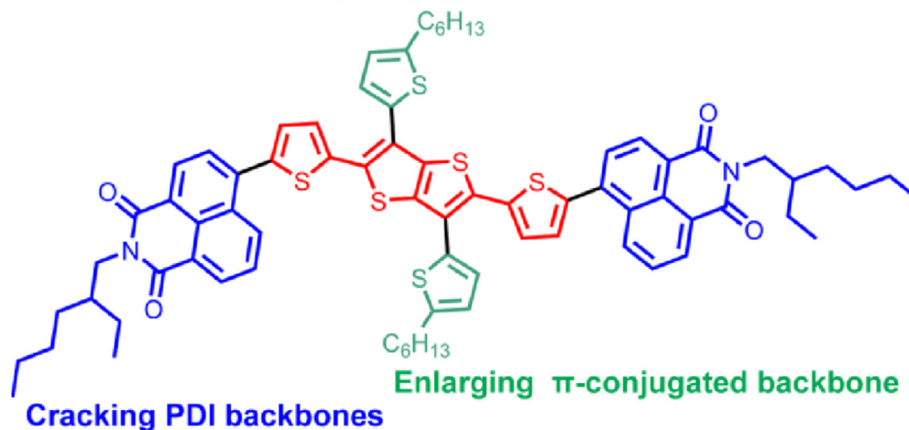
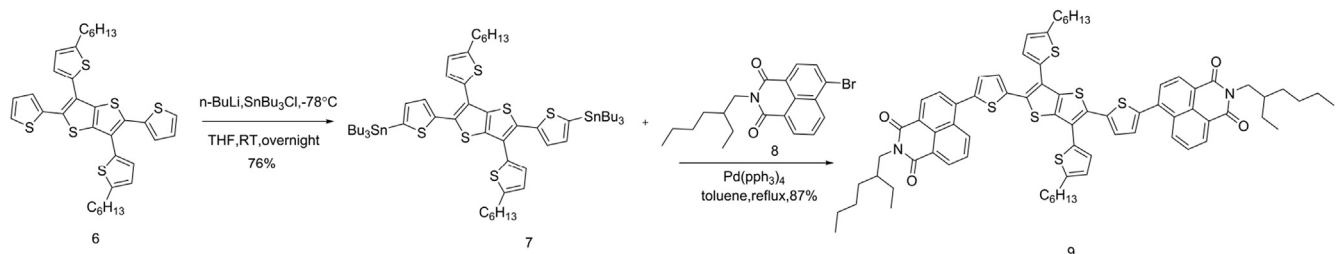
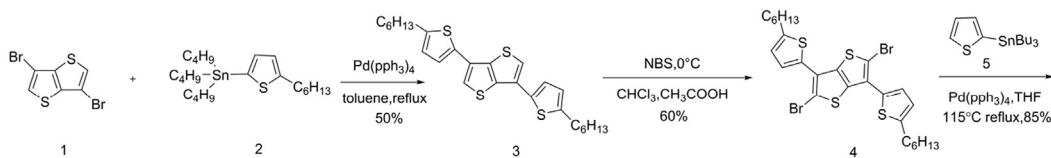


Chart 4. Schematic representation of the design of DNIT-TT2T.



Scheme 4. Synthetic routes of compound DNIT-TT2T.

NMR (CDCl_3 , 300 MHz): δ 8.67 (dd, $J = 7.3, 6.1$ Hz, 4H), 8.59 (d, $J = 7.6$ Hz, 2H), 7.79 (m, 4H), 7.34 (d, $J = 3.8$ Hz, 2H), 7.27 (d, $J = 2.9$ Hz, 2H), 7.17 (d, $J = 3.5$ Hz, 2H), 6.82 (d, $J = 3.5$ Hz, 2H), 4.14 (m, 4H), 2.86 (t, $J = 7.6$ Hz, 4H), 1.96 (m, 2H), 1.70 (dd, $J = 15.2, 7.6$ Hz, 4H), 1.32 (m, 28H), 0.90 (m, 18H). ^{13}C NMR (CDCl_3 , 300 MHz): δ 164.49, 164.22, 147.89, 141.00, 138.37, 138.06, 132.30, 132.07, 131.73, 131.42, 130.64, 129.70, 129.00, 128.85, 128.41, 128.21, 127.77, 127.21, 125.47, 124.50, 122.98, 122.01, 44.18, 37.88, 31.50, 31.48, 30.71, 30.18, 28.71, 28.67, 24.02, 23.03, 22.50, 14.06, 14.01, 10.62. IR (KBr), cm^{-1} : 2956, 2926, 2855, 1700, 1660, 1587, 1512, 1462, 1432, 1385, 1354, 1233, 1182, 1097, 859, 801, 783, 756. HRMS (+ESI), m/z calcd. for $\text{C}_{74}\text{H}_{78}\text{N}_2\text{O}_4\text{S}_6$ ($\text{M}+\text{H})^+$ 1251.4286, found 1251.4331. Anal. calc. For $\text{C}_{74}\text{H}_{78}\text{N}_2\text{O}_4\text{S}_6$: C, 71.00; H, 6.28; N, 2.24. Found: C, 70.42; H, 6.18; N, 2.17.

Compound 7 was obtained by slowly adding n-Butyllithium (0.47 ml, 1.6 mol/L in hexane) to a 50 ml flask filled with a solution of **compound 6** in dry THF (16.7 ml), at -78°C under nitrogen, and then the mixture was stirred at -78°C for 2 h. Then the solution of SnBu_3Cl was added and it was allowed to attain the room temperature. After stirring for 24 h, water was added and the mixture was extracted with diethyl ether for three times. The organic phase was washed with brine and dried over anhydrous magnesium sulfate. The solvent was removed by rotary evaporation and the crude product was obtained as a yellow oil (1 g, 76%). It was used

directly in the next step without further purification.

Compound 6 was synthesized according to the same procedure as for **compound 3**. **Compound 4** (0.5 g, 0.8 mmol), **compound 5** (0.9 g, 2.4 mmol), anhydrous toluene (4 ml), tetrakis(-triphenylphosphine)palladium (0) [$\text{Pd}(\text{pph}_3)_4$] (18 mg, 0.016 mmol) were used. The crude product was purified by column chromatograph using petroleum ether as eluent to give **compound 6** as a yellow solid (85%). ^1H NMR (CDCl_3 , 300 MHz): δ 7.33 (dd, $J = 5.1, 1.1$ Hz, 2H), 7.19 (dd, $J = 3.6, 1.1$ Hz, 2H), 7.06–7.00 (m, 4H), 6.74 (d, $J = 3.6$ Hz, 2H), 2.81 (t, $J = 7.6$ Hz, 4H), 1.67 (dd, $J = 14.4, 6.8$ Hz, 4H), 1.42–1.27 (m, 12H), 0.89 (t, $J = 6.3$ Hz, 6H).

Compound 4 was synthesized by dissolving **Compound 3** (5 g, 10.6 mmol) in a mixed solvent of chloroform and glacial acid (3:1 by vol.) at 0°C in dark under a nitrogen atmosphere. NBS (3.77 g, 21 mmol) was added to the reaction mixture and allowed to react for 5 h at 0°C . The solution was then poured into deionized water and extracted with chloroform. The organic extract was dried over anhydrous magnesium sulfate and evaporated to remove the solvent. The crude product was washed with hexane several times to give a light solid. This crude product was then finally purified by column chromatograph using petroleum ether as eluent to give **compound 4** as a white solid (60%). ^1H NMR (CDCl_3 , 300 MHz): δ 7.39 (d, $J = 3.6$ Hz 2H), 6.84 (d, $J = 3.6$ Hz 2H), 2.86 (t, $J = 7.7$ Hz 4H), 1.72 (dd, $J = 15.2, 7.6$ Hz 4H), 1.34 (m, 12H), 0.91 (t, $J = 6.9$ Hz,

6H).

Compound 3 was synthesized by the following method: In a dry 500 ml flask, the **compound 1**(12 g, 40 mmol) and **compound 2** (85 g, 180 mmol) was dissolved in 200 ml anhydrous toluene and the solution was purged with nitrogen for 15 min. Then tetrakis(-triphenylphosphine)palladium (0) [Pd(pph₃)₄] (0.42 g, 0.36 mmol) was added under nitrogen. The mixture was vigorously stirred at 115 °C overnight under N₂ atmosphere and cooled down to room temperature. Water was added and the mixture was extracted with dichloromethane for three times, the combined organic phase was washed with brine and dried over anhydrous magnesium sulfate and evaporated to dryness. The crude product was purified by column chromatograph using petroleum ether as eluent to give **compound 3** as a colorless solid(50%). ¹H NMR (CDCl₃, 300 MHz): δ 7.44 (s, 2H), 7.20 (d, *J* = 2.7 Hz 2H), 6.78 (d, *J* = 1.5 Hz 2H), 2.84 (t, *J* = 5.7 Hz 4H), 1.72 (dt, *J* = 15.3, 7.5 Hz 4H), 1.34 (m, 12H), 0.91 (m, 6H).

3. Results and discussion

3.1. Thermal stability and optical absorption

DNIT-TT2T shows good solubility in common organic solvents such as dichloromethane (CH₂Cl₂), chloroform (CHCl₃), and o-dichlorobenzene (DCB) at room temperature.

To better understand the thermal properties of the molecule, thermogravimetric analysis (TGA) was carried out (see ESI, Fig. S1). **DNIT-TT2T** exhibits an excellent thermal stability with decomposition temperature (*T_d*) of 450 °C at 5% weight loss under an atmosphere of nitrogen, which indicates that the thermal stability of **DNIT-TT2T** is high enough for practical application in organic photovoltaic.

In order to study the relationship between the chemical structure and the photophysical properties, Fig. 1 (a) shows the normalized UV-vis absorption spectra of **DNIT-TT2T** in diluted chloroform solution at a concentration of 2.16 × 10⁻⁵ M and in thin solid films prepared by spin-coating. The material displays a broad absorption in the wavelength range of 300 nm–600 nm and two absorption peaks are mainly observed at 360 nm and 448 nm respectively in solution. Compound **DNIT-TT2T** has a shoulder at ca.350 nm, which is assigned to the naphthalimide [70], the other absorption peaks in the longer wavelength region are attributed to intramolecular charge transfer (ICT) interaction between the donor unit and acceptor

groups NI [71]. **DNIT-TT2T** exhibits absorption coefficients of 4.22 × 10⁴ M⁻¹ cm⁻¹ (360 nm) and 3.99 × 10⁴ M⁻¹ cm⁻¹ (448 nm) in chloroform solution. **DNIT-TT2T** in thin film exhibits broader absorption with a similar profile and significant red-shift relative to that in solution, suggesting that there is better molecular aggregation and a strong intermolecular interaction in the thin film. The optical band gap estimated from the absorption edge of the thin films is 2.19 eV. Moreover, the blend film with P3HT (1:1 w/w) exhibit broad absorption ranging from 300 to 700 nm (Fig. 1a).

3.2. Electrochemical properties and energy levels

The electrochemical properties of the compound were investigated by electrochemical cyclic voltammetry (CV) of thin films deposited on a glassy carbon working electrode in 0.1 M TBAPF₆ solution of CH₃CN at a potential scan rate of 100 mV s⁻¹, and the ferrocene/ferrocenium (Fc/Fc⁺) redox couple was used to calibrate the potentials under the same experimental conditions. **DNIT-TT2T** showed irreversible p-doping process. As shown in Fig. 1b, the onset oxidation potential (E_{ox}) is 0.92 V versus Ag/Ag⁺ reference electrode. The HOMO energies were calculated from the onset oxidation potentials according to equation E = -(E_{ox.onset} - E_{Fe/Fe+} + 5.1) (eV). As shown in Table 1, the large HOMO energy offset between **DNIT-TT2T** and P3HT (-5.1 eV) ensures efficient hole transfer from acceptor to donor. LUMO levels were determined based on the relationship E_{LUMO} = E_{HOMO} + E_g^{opt}. **DNIT-TT2T** exhibits a high LUMO energy level (-3.75 eV), which would reduce the energy loss when blended with the donor possessing a high LUMO level. The low-lying HOMO level of donor and the high-lying LUMO level of acceptor would give rise to a high V_{oc} for non-fullerene PSCs [72].

Table 1
Electrochemical and optical properties of DNIT-TT2T.

	λ_{max} (nm)		E_g^{opt} (eV) ^a	HOMO(eV) ^b	LUMO(eV) ^c
	solution	Film			
DNIT-TT2T	360,350 sh ^d ,448	362,460	2.19	-5.94	-3.75

^a Calculated by the equation: $E_g^{\text{opt}} = 1240/\lambda_{\text{onset}}$.

^b Determined by the CV test.

^c Determined by the equation: E_{LUMO} = E_{HOMO} + E_g^{opt}.

^d Shoulder.

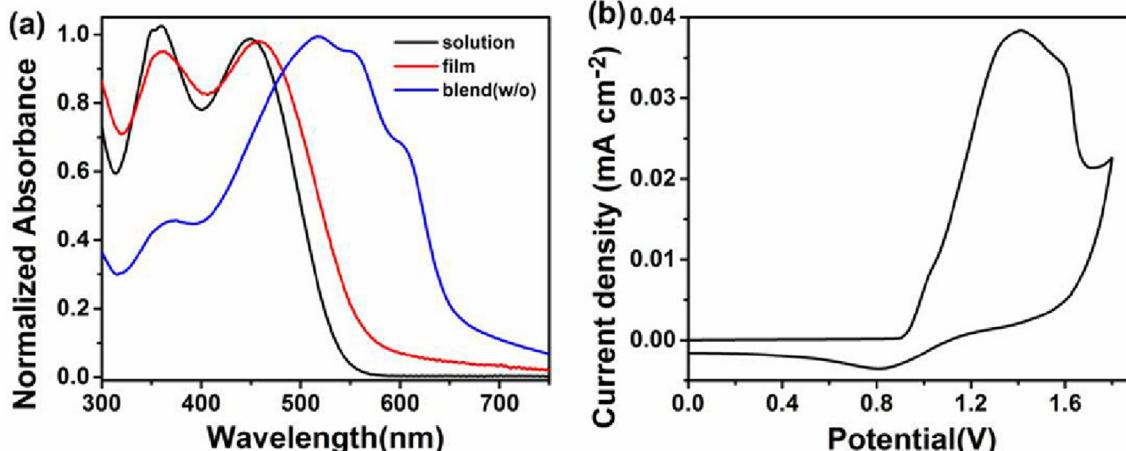


Fig. 1. (a) UV-vis absorption spectra of DNIT-TT2T in chloroform solution, thin solid film state, and the blend film of P3HT:DNIT-TT2T(1:1); (b) Cyclic voltammograms of DNIT-TT2T as thin films on glassy carbon working electrodes.

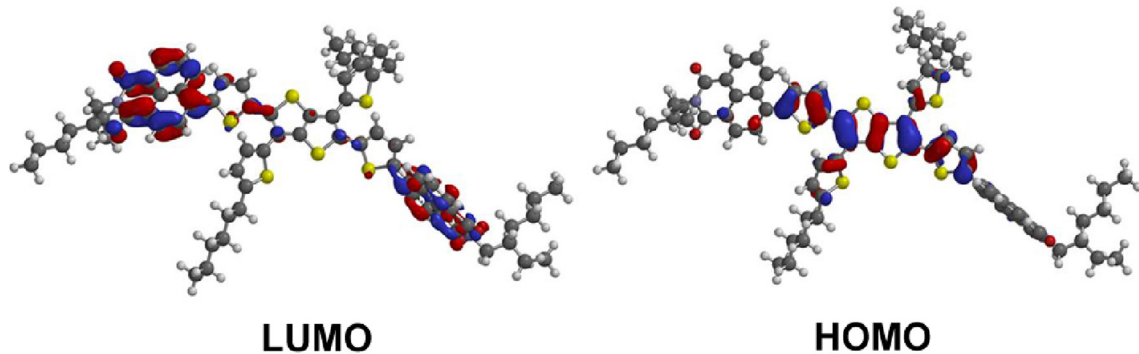


Fig. 2. Frontier molecular orbits of DINIT-TT2T based on the optimized geometries (calculated using DFT performed by Spartan).

3.3. Theoretical calculations

In order to shed light on the ground-state molecular configuration and electronic structures of **DNIT-TT2T**, computational studies were performed by density functional theory (DFT). As shown in Fig. 2, we can see the optimized geometries and the electron distributions of HOMO and LUMO levels of **DNIT-TT2T**. The HOMO energy level is mainly delocalized on the thiophene and thiophene units, on the other hand, the LUMO energy level is mainly located on the NI moiety, because thiophene and thiophene act as donor and NI acts as acceptor in this A-D-A structure. The calculated band gap of optimized ground-state geometry of **DNIT-TT2T** is 2.77 eV and the trend in the

experimentally estimated band gap is consistent with that of the theoretically estimated values.

3.4. Photovoltaic properties

In order to evaluate the potential of **DNIT-TT2T**, as a novel non-fullerene acceptor material, the devices with structure ITO/PEDOT:PSS (40 nm)/P3HT:DNIT-TT2T (80 nm)/Ca (10 nm)/Al (90 nm) were fabricated (Fig. 3a). Representative current density-voltage (*J-V*) curves of the devices under the light intensity 100 mW cm⁻² are shown in Fig. 3c, and the corresponding parameters are summarized in Table 2. (The performance of devices based on different ratio of P3HT:DNIT-TT2T is displayed in Table S2

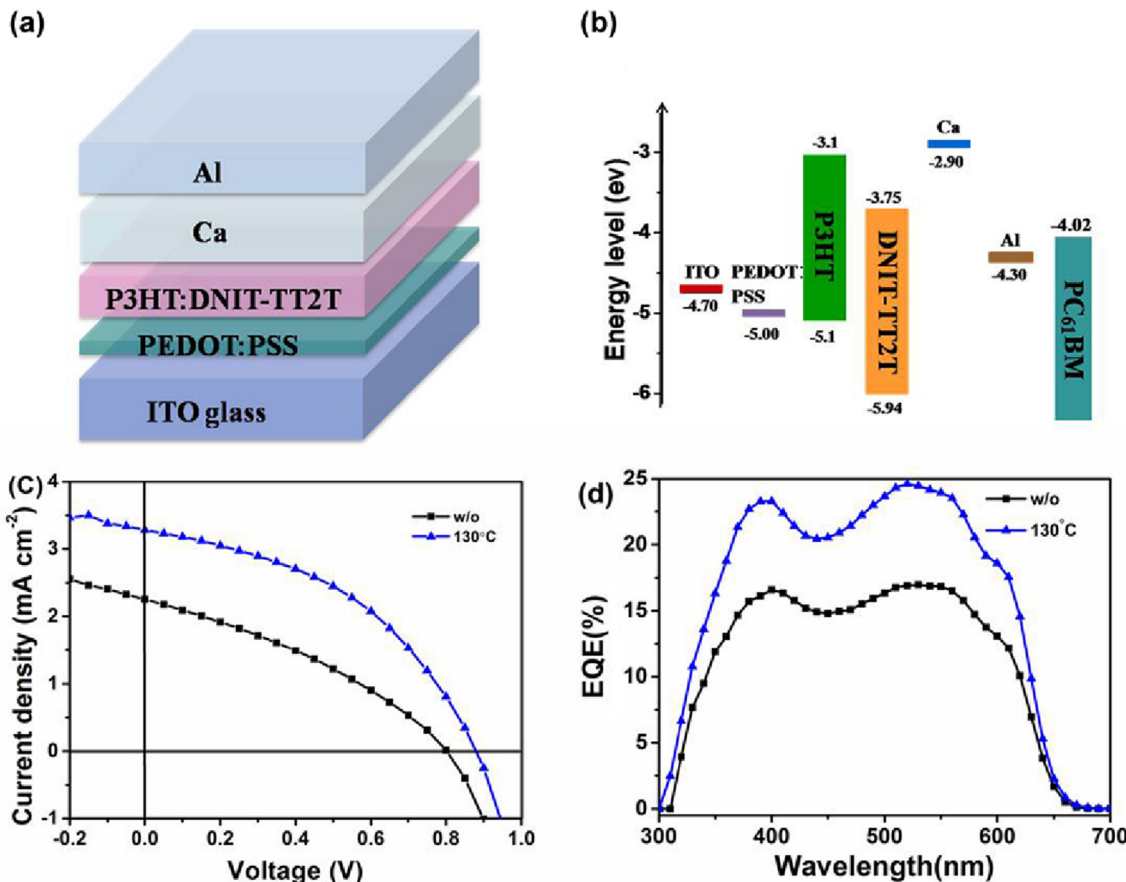


Fig. 3. (a) The structure of the devices; (b) energy level diagram of materials; (c) current density–voltage (J - V) and (d) EQE curves of the OSC devices.

Table 2

Photovoltaic performance of the PSCs under illumination of 100 mW cm^{-2} for the devices with a structure of ITO/PEDOT:PSS (40 nm)/P3HT:DNI-TT2T (80 nm)(ratio 1:1)/Ca (10 nm)/Al (90 nm).

P3HT:DNI-TT2T = 1:1 (Thermal annealing temperature)	V_{oc} (V)	J_{sc} (mA cm^{-2})	FF (%)	PCE (%)
w/o	0.80	2.25	34.08	0.62
130 °C 10 min	0.88	3.28	43.47	1.25

Table 3

OPV properties of P3HT.

Acceptor	D:A ratio(w/w)	V_{oc} [V]	J_{sc} [mA cm^{-2}]	FF	PCE _{max} [%]	Ref
PC ₆₁ BM	1:1	0.66	6.74	0.68	3.04	This work
BTz-Np	1:1	0.94	3.52	0.46	1.53	[74]
NTz-Np	1:1	0.90	5.18	0.60	2.81	[74]
Ph-D	1:1	0.51	1.03	0.31	0.16	[75]
Ph-EH	1:1	0.89	3.99	0.45	1.58	[75]
Ph-MH	1:1	0.76	5.59	0.48	2.05	[75]
Ph-Ipop	1:1	0.66	0.55	0.29	0.11	[75]
Th-EH	1:1	0.72	1.44	0.36	0.38	[75]
IDT-2DPP	1:1.2	1.17	1.43	0.50	0.83	[36]
IDT-2PDI	1:1	0.69	3.07	0.51	1.08	[38]
O-IDTBR	1:1	0.72	13.9	0.60	6.40	[19]
EH-IDTBR	1:1	0.76	12.1	0.62	6.00	[19]
IDT-2BR	1:1	0.84	5.99	0.69	3.49	[39]

and Fig. S4).

Both the HOMO and LUMO of **DNI-TT2T** are significantly lower than those of P3HT (-3.1 and -5.1 eV), as depicted in Fig. 3b. The offset between the HOMO of P3HT and the LUMO of DNI-TT2T (1.35 eV) is much larger than that between the PC₆₁BM and P3HT (1.08 eV) which is beneficial to obtain a high V_{oc} (>0.8 V) for polymer solar cells based on P3HT and **DNI-TT2T** compared with the devices based on the donor material P3HT and a series of non-fullerene acceptors (see ESI, Fig. S2, Table S1 and Table 3). Moreover, there is sufficient driving force to promote the separation of excitons. The device performance was optimized by varying the annealing temperature. From Table 2, the V_{oc} of the devices annealed at 130 °C is greatly improved (0.08 V), as explained in Fig. 4 which shows that the decrease in J_{sc} can increase the V_{oc} of the device [73]. To get a better understanding of the device performance, the external quantum efficiency (EQE) spectra of the devices were measured and depicted in Fig. 3d. The devices show a

broad solar spectral response in the wavelength range of 300–650 nm, which demonstrates that both P3HT polymer donor and **DNI-TT2T** acceptor contribute to generate excitons. J_{sc} value of the device with the highest PCE (1.25%) calculated from integrated EQE curves is 3.317 mA cm^{-2} , which has only 1.1% mismatch with that obtained from $J-V$ measurements. Moreover, the PCE is almost comparable with that of P3HT based solar cells (Table 3).

3.5. Film morphology

The morphology of the active layers has a tremendous impact on the photovoltaic performance of OPVs. The active layer morphology of P3HT/DNI-TT2T (1:1 ratio) blended films spin-coated from o-dichlorobenzene solution was characterized by AFM in the tapping-mode as shown in Fig. 5. The root-mean-square (RMS) roughness of the as casted films (w/o) and those annealed at 130 °C is 2.04 and 5.11 nm, respectively. After annealing, the RMS roughness of the blend films increases, meaning better phase separation which is beneficial for the exciton separation and charge transportation in the active layer, leading to higher J_{sc} , FF and PCE [43,76].

4. Conclusion

The fused-ring electron acceptors were discussed and non-fullerene acceptor design strategy was proposed. Based on this, a new non-fullerene acceptor (DNI-TT2T) was designed, synthesized and characterized. This material exhibits good solubility in common solvents, good thermal stability, a strong absorption in the visible region, and appropriate energy levels match with the commonly used polymer donor P3HT. Compared to PC₆₁BM, DNI-TT2T exhibits higher LUMO level reducing the gap of LUMO levels between donor and acceptor. Solution-processed OSCs based on DNI-TT2T acceptor exhibit the PCE of 1.25% with a J_{sc} of 3.28 mA cm^{-2} , high V_{oc} of 0.88 V and FF of 43.47%. These results demonstrate that NI based small molecule is a promising alternative of fullerene, and a more excellent photovoltaic performance could be expected by optimizing the devices. It also provides a novel idea to develop non-fullerene acceptors for future organic electronics applications.

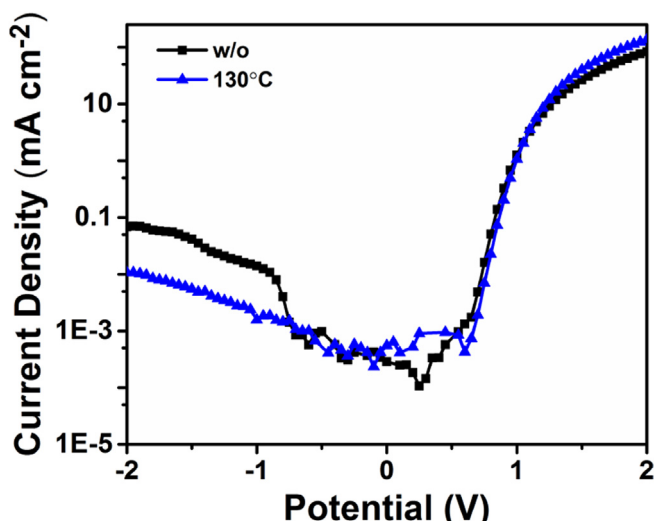


Fig. 4. Semi-logarithmic current density vs. voltage characteristics of the devices in the dark.

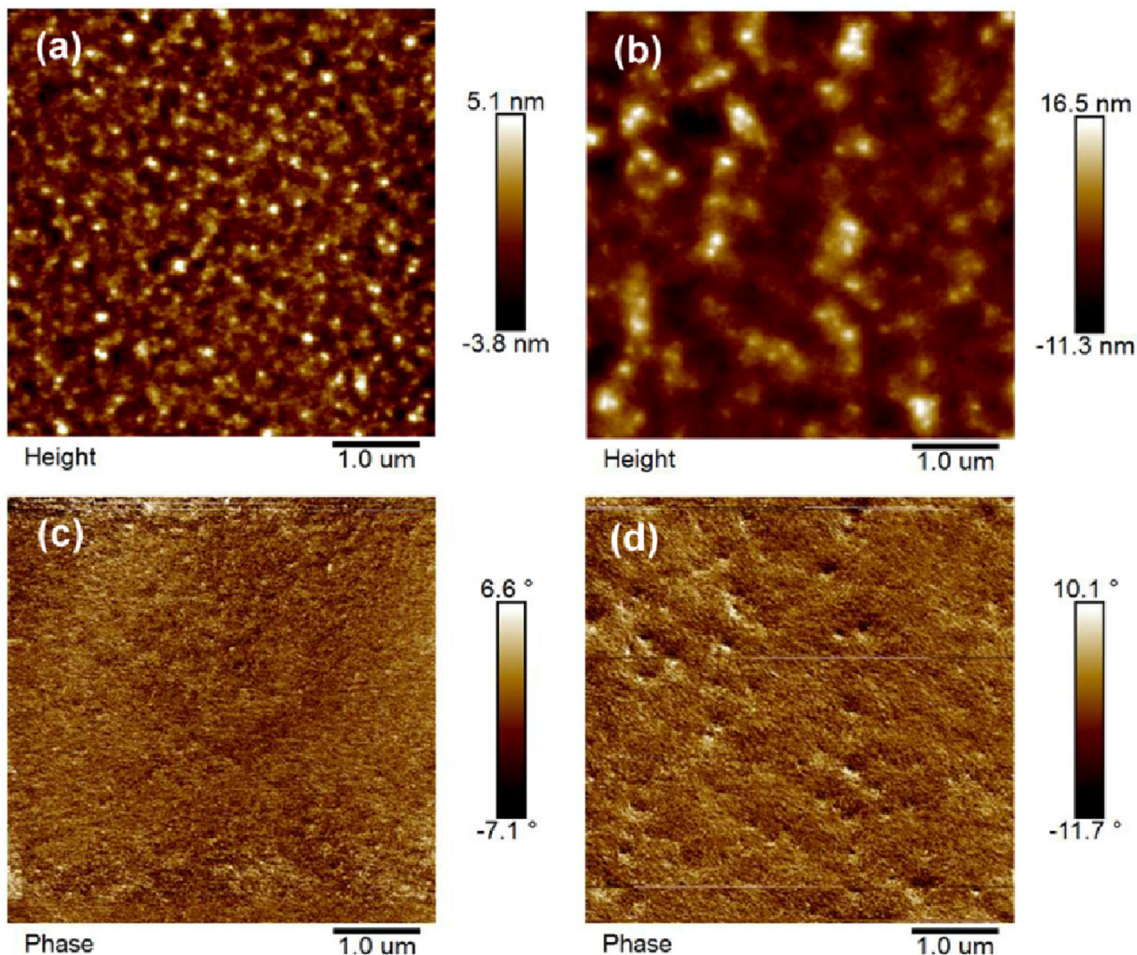


Fig. 5. Tapping mode AFM topography height images ($5 \times 5 \mu\text{m}^2$) of the blend films of P3HT:DNIT-TT2T, (a) as cast (w/o) (b) annealed at 130°C for 10 min; phase images of the blend films of P3HT:DNIT-TT2T, (c) as cast (w/o) (d) annealed at 130°C for 10 min.

Acknowledgements

This work was financially supported by the Shenzhen Peacock Plan (KQTD2014062714543296), Shenzhen Science and Technology Research Grant (JCYJ20160510144254604), National Basic Research Program of China (973 Program, No. 2015CB856505), Natural Science Foundation of Guangdong Province (2014A030313800), Guangdong Academician Workstation and Guangdong Talents Project.

Appendix A. Supplementary data

Supplementary data related to this article can be found at <http://dx.doi.org/10.1016/j.dyepig.2017.03.015>.

References

- [1] Cheng YJ, Yang SH, Hsu CS. Synthesis of conjugated polymers for organic solar cell applications. *Chem Rev* 2009;109(11):5868–923.
- [2] Li YF. Molecular design of photovoltaic materials for polymer solar cells: toward suitable electronic energy levels and broad absorption. *Acc Chem Res* 2012;45(5):723–33.
- [3] Krebs FC. Fabrication and processing of polymer solar cells: a review of printing and coating techniques. *Sol Energy Mater Sol Cells* 2009;93(4):394–412.
- [4] Lu LY, Zheng TY, Wu QH, Schneider AM, Di Zhao, Yu LP. Recent advances in bulk heterojunction polymer solar cells. *Chem Rev* 2015;115(23):12666–731.
- [5] Bin HJ, Zhang ZG, Gao L, Chen SS, Zhong L, Xue LW, et al. Non-fullerene polymer solar cells based on alkylthio and fluorine substituted 2d-conjugated polymers reach 9.5% efficiency. *J Am Chem Soc* 2016;138(13):4657–64.
- [6] Li G, Zhu R, Yang Y. Polymer solar cells. *Nat Phot* 2012;6(3):153–61.
- [7] Zhang JQ, Zhang YJ, Fang J, Lu K, Wang ZY, Ma W, et al. Conjugated polymer–small molecule alloy leads to high efficient ternary organic solar cells. *J Am Chem Soc* 2015;137(25):8176–83.
- [8] Zhou HQ, Zhang Y, Mai CK, Collins SD, Bazan GC, Nguyen TQ, et al. Polymer Homo-Tandem solar cells with best efficiency of 11.3%. *Adv Mater* 2015;27(10):1767–73.
- [9] Zhang SQ, Ye L, Zhao WC, Yang B, Wang Q, Hou JH. Realizing over 10% efficiency in polymer solar cell by device optimization. *Sci China Chem* 2015;58(2):248–56.
- [10] Gu C, Huang N, Chen YC, Zhang HH, Zhang ST, Li FH, et al. Porous organic polymer films with tunable work functions and selective hole and electron flows for energy conversions. *Angew Chem Int Ed* 2016;55(9):3049–53.
- [11] Gu C, Chen YC, Zhang ZB, Xue SF, Sun SH, Zhong CM, et al. Achieving high efficiency of PTB7-based polymer solar cells via integrated optimization of both anode and cathode interlayers. *Adv Energy Mater* 2014;4(9):1301771.
- [12] Gu C, Huang N, Youchun Chen, Qin LQ, Xu H, Zhang ST, et al. p-Conjugated microporous polymer films: designed synthesis, conducting properties, and photoenergy conversions. *Angew Chem Int Ed* 2015;54(46):13594–8.
- [13] Gu C, Chen YC, Zhang ZB, Xue SF, Sun SH, Zhang K, et al. Electrochemical route to fabricate film-like conjugated microporous polymers and application for organic electronics. *Adv Mater* 2013;25(25):3443–8.
- [14] Anttil A, Babbitt CW, Raffaelle RP, Landi BJ. Material and energy intensity of fullerene production. *Environ Sci Technol* 2011;45(6):2353–9.
- [15] He YJ, Chen HY, Hou JH, Li YF. Indene-C60 bisadduct: a new acceptor for high-performance polymer solar cells. *J Am Chem Soc* 2010;132(4):1377–82.
- [16] Lin YZ, He Q, Zhao FW, Huo LJ, Mai JQ, Lu XH, et al. A facile planar fused-ring electron acceptor for as-cast polymer solar cells with 8.71% efficiency. *J Am Chem Soc* 2016;138(9):2973–6.
- [17] Li SS, Zhang H, Zhao WC, Ye L, Yao HF, Yang B, et al. Green-solvent-processed all-polymer solar cells containing a perylene diimide-based acceptor with an efficiency over 6.5%. *Adv Energy Mater* 2016;6(5):1501991.
- [18] Lin YZ, Zhao FW, He Q, Huo LJ, Wu Y, Parker TC, et al. High-performance

- electron acceptor with thiényl side chains for organic photovoltaics. *J Am Chem Soc* 2016;138(14):4955–61.
- [19] Holliday S, Ashraf RS, Wadsworth A, Baran D, Yousaf SA, Nielsen CB, et al. High-efficiency and air-stable P3HT-based polymer solar cells with a new non-fullerene acceptor. *Nat Commun* 2016;7:11585.
- [20] Meng D, Sun D, Zhong CM, Liu T, Fan BB, Huo LJ, et al. High-performance solution-processed non-fullerene organic solar cells based on selenophene-containing perylene bisimide acceptor. *J Am Chem Soc* 2016;138(1):375–80.
- [21] Zhong Y, Trinh MT, Chen RS, Purdum GE, Khlyabich PP, Sezen M, et al. Molecular helices as electron acceptors in high-performance bulk heterojunction solar cells. *Nat Commun* 2015;6:8242.
- [22] Lin YZ, He Q, Zhao FW, Huo LJ, Mai JQ, Lu XH, et al. A facile planar fused-ring electron acceptor for as-cast polymer solar cells with 8.71% efficiency. *J Am Chem Soc* 2016;138(9):2973–6.
- [23] Bin HJ, Zhang ZG, Gao L, Chen SS, Zhong L, Xue LW, et al. Non-fullerene polymer solar cells based on alkylthio and fluorine substituted 2d-conjugated polymers reach 9.5% efficiency. *J Am Chem Soc* 2016;138(13):4657–64.
- [24] Holliday S, Ashraf RS, Nielsen CB, Kirkus M, Röhr JA, Tan CH, et al. A rhodanine flanked nonfullerene acceptor for solution-processed organic photovoltaics. *J Am Chem Soc* 2015;137(2):898–904.
- [25] Wu CH, Chueh CC, Xi YY, Zhong HL, Gao GP, Wang ZH, et al. Influence of molecular geometry of perylene diimide dimers and polymers on bulk heterojunction morphology toward high-performance nonfullerene polymer solar cells. *Adv Funct Mater* 2015;25(33):5326–32.
- [26] Gao L, Zhang ZG, Xue L, Min J, Zhang JQ, Wei ZX, et al. All-polymer solar cells based on absorption-complementary polymer donor and acceptor with high power conversion efficiency of 8.27%. *Adv Mater* 2016;28(9):1884–90.
- [27] Lin YZ, Wang JY, Zhang ZG, Bai HT, Li YF, Zhu DB, et al. An electron acceptor challenging fullerenes for efficient polymer solar cells. *Adv Mater* 2015;27(7):1170–4.
- [28] Li SX, Liu WQ, Shi MM, Mai JQ, Lau TK, Wan JH, et al. A spirobifluorene and diketopyrrolopyrrole moieties based non-fullerene acceptor for efficient and thermally stable polymer solar cells with high open-circuit voltage. *Energy Environ Sci* 2016;9(2):604–10.
- [29] Liu F, Zhou ZC, Zhang C, Vergote T, Fan HJ, Liu F, et al. A thieno[3,4-b]thiophene-based non-fullerene electron acceptor for high-performance bulk-heterojunction organic solar cells. *J Am Chem Soc* 2016;138(48):15523–6.
- [30] Zhao WC, Qian DP, Zhang SQ, Li SS, Inganäs O, Gao F, et al. Fullerene-Free polymer solar cells with over 11% efficiency and excellent thermal stability. *Adv Mater* 2016;28(23):4734–9.
- [31] Qin YP, Uddin MA, Chen Y, Jang B, Zhao K, Zheng Z, et al. Highly efficient fullerene-free polymer solar cells fabricated with polythiophene derivative. *Adv Mater* 2016;28(42):9416–22.
- [32] Zhang SQ, Qin YP, Uddin MA, Jang B, Zhao WC, Liu DL, et al. A fluorinated polythiophene derivative with stabilized backbone conformation for highly efficient fullerene and non-fullerene polymer solar cells. *Macromolecules* 2016;49(8):2993–3000.
- [33] Gao L, Zhang ZG, Bin HJ, Xue LW, Yang YK, Wang C, et al. High-efficiency nonfullerene polymer solar cells with medium bandgap polymer donor and narrow bandgap organic semiconductor acceptor. *Adv Mater* 2016;28(37):8288–95.
- [34] Li SS, Ye L, Zhao WC, Zhang SQ, Mukherjee S, Ade H, et al. Energy-level modulation of small-molecule electron acceptors to achieve over 12% efficiency in polymer solar cells. *Adv Mater* 2016;28(42):9423–9.
- [35] Li YX, Liu XD, Wu FP, Zhou Y, Jiang ZQ, Song B, et al. Non-fullerene acceptor with low energy loss and high external quantum efficiency: towards high performance polymer solar cells. *J Mater Chem A* 2016;4(16):5890–7.
- [36] Yang YK, Zhang ZG, Bin HJ, Chen SS, Gao L, Xue LW, et al. Side-chain isomerization on an n-type organic semiconductor ITIC acceptor makes 11.77% high efficiency polymer solar cells. *J Am Chem Soc* 2016;138(45):15011–8.
- [37] Qiu NL, Zhang HJ, Wan XJ, Li CX, Ke X, Feng HR, et al. A new nonfullerene electron acceptor with a ladder type backbone for high-performance organic solar cells. *Adv Mater* 2016;29(6):1604964.
- [38] Bai HT, Cheng P, Wang YF, Ma LC, Li YF, Zhu DB, et al. A bipolar small molecule based on indacenodithiophene and diketopyrrolopyrrole for solution processed organic solar cells. *J Mater Chem A* 2014;2(3):778–84.
- [39] Bai HT, Wang YF, Cheng P, Wang JY, Wu Y, Hou JH, et al. An electron acceptor based on indacenodithiophene and 1,1-dicyanomethylene-3-indanone for fullerene-free organic solar cells. *J Mater Chem A* 2015;3(5):1910–4.
- [40] Lin YZ, Wang JY, Dai SX, Li YF, Zhu DB, Zhan XW. A twisted dimeric perylene diimide electron acceptor for efficient organic solar cells. *Adv Energy Mater* 2014;4(13):1400420.
- [41] Wu Y, Bai HT, Wang ZY, Cheng P, Zhu SY, Wang YF, et al. A planar electron acceptor for efficient polymer solar cells. *Energy Environ Sci* 2015;8(11):3215–21.
- [42] Lin YZ, Zhang ZG, Bai HT, Wang JY, Yao YH, Li YF, et al. High-performance fullerene-free polymer solar cells with 6.31% efficiency. *Energy Environ Sci* 2015;8(2):610–6.
- [43] Yao HF, Chen Y, Qin YP, Yu RN, Cui Y, Yang B, et al. Design and synthesis of a low bandgap small molecule acceptor for efficient polymer solar cells. *Adv Mater* 2016;28(37):8283–7.
- [44] Li YX, Zhong L, Wu FP, Yuan Y, Bin HJ, Jiang ZQ, et al. Non-fullerene polymer solar cells based on a selenophene-containing fused-ring acceptor with photovoltaic performance of 8.6%. *Energy Environ Sci* 2016;9(11):3429–35.
- [45] Wurthner F. Perylene bisimide dyes as versatile building blocks for functional supramolecular architectures. *Chem Commun* 2004;14:1564–79.
- [46] Shin WS, Jeong HH, Kim MK, Jin SH, Kim MR, Lee JK, et al. Effects of functional groups at perylene diimide derivatives on organic photovoltaic device application. *J Mater Chem* 2006;16(4):384–90.
- [47] Hartnett PE, Matte HSSR, Eastham ND, Jackson NE, Wu YL, Chen LX, et al. Ring-fusion as a perylenediimide dimer design concept for high-performance non-fullerene organic photovoltaic acceptors. *Chem Sci* 2016;7(6):3543–55.
- [48] Zhang X, Zhan CL, Yao JN. Non-fullerene organic solar cells with 6.1% efficiency through fine-tuning parameters of the film-forming process. *Chem Mater* 2015;27(1):166–73.
- [49] Huang C, Barlow S, Marder SR. Perylene-3,4,9,10-tetracarboxylic acid diimides: synthesis, physical properties, and use in organic electronics. *J Org Chem* 2011;76(8):2386–407.
- [50] Zhou Y, Kuroswa T, Ma W, Guo YK, Fang L, Vandewal K, et al. High performance all-polymer solar cell via polymer side-chain engineering. *Adv Mater* 2014;26(22):3767–72.
- [51] Cheng P, Ye L, Zhao XG, Hou JH, Li YF, Zhan XW. Binary additives synergistically boost the efficiency of all-polymer solar cells up to 3.45%. *Energy Environ Sci* 2014;7(4):1351–6.
- [52] Zhao DL, Wu QH, Cai ZX, Zheng TY, Chen W, Lu J, et al. Electron acceptors based on α -substituted perylene diimide (PDI) for organic solar cells. *Chem Mater* 2016;28(4):1139–46.
- [53] Hadmojo WT, Nam SY, Shin TJ, Yoon SC, Jang SY, Jung IH. Geometrically controlled organic small molecule acceptors for efficient fullerene-free organic photovoltaic devices. *J Mater Chem A* 2016;4(31):12308–18.
- [54] Zhong HL, Wu CH, Li CZ, Carpenter J, Chueh CC, Chen JV, et al. Rigidifying nonplanar perylene diimides by ring fusion toward geometry-tunable acceptors for high-performance fullerene-free solar cells. *Adv Mater* 2016;28(5):951–8.
- [55] Zhang XJ, Zhang JC, Lu H, Wu JY, Li GW, Li CH, et al. A 1,8-naphthalimide based small molecular acceptor for polymer solar cells with high open circuit voltage. *J Mater Chem C* 2015;3(27):6979–85.
- [56] Zhang JC, Zhang XJ, Li GW, Xiao HM, Li WH, Xie SF, et al. A nonfullerene acceptor for wide band gap polymer based organic solar cells. *Chem Commun* 2016;52(3):469–72.
- [57] Kwon OK, Park JH, Kim DW, Park SK, Park SY. An all-small-molecule organic solar cell with high efficiency nonfullerene acceptor. *Adv Mater* 2015;27(11):1951–6.
- [58] Zhang JC, Xiao HM, Zhang XJ, Wu Y, Li GW, Li CH, et al. 1,8-Naphthalimide-based nonfullerene acceptors for wide optical band gap polymer solar cells with an ultrathin active layer thickness of 35 nm. *J Mater Chem C* 2016;4(24):5656–63.
- [59] Jin ZN, Li NJ, Wang CF, Jiang HJ, Lu JM, Zhou QZ. Synthesis and fluorescence property of some novel 1,8-naphthalimide derivatives containing a thiophene ring at the C-4 position. *Dyes Pigments* 2013;96(1):204–10.
- [60] Hou R, Feng SY, Gong X, Liu YH, Zhang JC, Li CH, et al. Side chain effect of nonfullerene acceptors on the photovoltaic performance of wide band gap polymer solar cells. *Synth Met* 2016;220:578–84.
- [61] Hamaguchi A, Negishi T, Kimura Y, Ikeda Y, Takimiya K, Bisri SZ, et al. Single-crystal-like organic thin-film transistors fabricated from dinaphtho[2,3-b:2',3'-f]thieno[3,2-b]thiophene (DNNT) precursor-polystyrene blends. *Adv Mater* 2015;27(42):6606–11.
- [62] Zhang Q, Wang YC, Kan B, Wan XJ, Liu F, Ni W, et al. A solution-processed high performance organic solar cell using a small molecule with the thieno[3,2-b]thiophene central unit. *Chem Commun* 2015;51(83):15268–71.
- [63] Turkoglu G, Cinar ME, Buyruk A, Tekin E, Mucur SP, Kaya K, et al. Novel organoboron compounds derived from thieno[3,2-b]thiophene and triphenylamine units for OLED devices. *J Mater Chem C* 2016;4(25):6045–53.
- [64] Kesarkar S, Mróz W, Penconi M, Pasini M, Destri S, Cazzaniga M, et al. Near-infrared emitting iridium(III) complexes with heteroaromatic β -diketonate ancillary ligands for efficient solution-processed OLEDs: structure–property correlations. *Angew Chem* 2016;128(8):2764–8.
- [65] Mao ZH, Senevirathna W, Liao JY, Gu J, Kesava SV, Guo CH, et al. Azadi-pyrromethene-based Zn(II) complexes as nonplanar conjugated electron acceptors for organic photovoltaics. *Adv Mater* 2014;26(36):6290–4.
- [66] Turbiez M, Frere P, Leriche P, Mercier N, Roncali J. Poly(3,6-dimethoxy-thieno[3,2-b]thiophene): a possible alternative to poly(3,4-ethylenedioxythiophene) (PEDOT). *Chem Commun* 2005;9:1161–3.
- [67] Kuo CY, Huang YC, Hsiow CY, Yang YW, Huang CI, Rwei SP, et al. Effect of side-chain architecture on the optical and crystalline properties of two-dimensional polythiophenes. *Macromolecules* 2013;46(15):5985–97.
- [68] Yu J, Shen TL, Weng WH, Huang YC, Huang CI, Su WF, et al. Molecular design of interfacial modifiers for polymer-inorganic hybrid solar cells. *Adv Energy Mater* 2012;2(2):245–52.
- [69] Wu WT, Wu XY, Zhao JZ, Wu MB. Synergistic effect of $C^{\bullet}N\cdot/C^{\bullet}N^{\bullet}$ coordination and the arylacetylidyne ligands on the photophysical properties of cyclometalated platinum complexes. *J Mater Chem C* 2015;3(10):2291–301.
- [70] He Q, Li TF, Yan CQ, Liu Y, Wang JY, Wang MG, et al. Cracking perylene diimide backbone for fullerene-free polymer solar cells. *Dyes Pigments* 2016;128:226–34.
- [71] Jespersen KG, Beenken WJD, Zaushitsyn Y, Yartsev A, Andersson M, Pullerits T, et al. The electronic states of polyfluorene copolymers with alternating donor-acceptor units. *J Chem Phys* 2004;121(24):12613–7.
- [72] Sullivan P, Collis GE, Rochford LA, Arantes JF, Kemppinen P, Jones TS, et al. An N-ethylated barbituric acid end-capped bithiophene as an electron-acceptor

- material in fullerene-free organic photovoltaics. *Chem Commun* 2015;51(28):6222–5.
- [73] He C, Zhong CM, Wu HB, Yang RQ, Yang W, Huang F, et al. Origin of the enhanced open-circuit voltage in polymer solar cells via interfacial modification using conjugated polyelectrolytes. *J Mater Chem* 2010;20(13):2617–22.
- [74] Chatterjee S, le Y, Karakawa M, Aso Y. Naphtho[1,2-c:5,6-c']bis[1,2,5]thiadiazole-containing π -conjugated compound: nonfullerene electron acceptor for organic photovoltaics. *Adv Funct Mater* 2016;26(8):1161–8.
- [75] Jinnai S, le Y, Karakawa M, Aerouts T, Nakajima Y, Mori S, et al. Electron-accepting π -conjugated systems for organic photovoltaics: influence of structural modification on molecular orientation at donor–acceptor interfaces. *Chem Mater* 2016;28(6):1705–13.
- [76] Lin YZ, Zhao FW, Wu Y, Chen K, Xia YX, Li GW, et al. Mapping polymer donors toward high-efficiency fullerene free organic solar cells. *Adv Mater* 2016;1604155.